

## Synthesis and structure of polycrystals $\text{MnCo}_2\text{O}_4\text{-GdCrO}_4$

**M.M. Mataev<sup>1</sup>, G.S. Patrin<sup>2</sup>, A.A. Meldeshov<sup>1</sup>, K.Zh. Seitbekova<sup>3</sup>, M.E. Zhaisanbaeva<sup>1\*</sup>**

<sup>1</sup>Kazakh National Women's Pedagogical University, Gogol str., 114 k1, Almaty, Kazakhstan

<sup>2</sup>Siberian Federal University, Svobodny ave., 79, Krasnoyarsk, Russia

<sup>3</sup>Abai Kazakh National Pedagogical University, Dostyk ave., 13, Almaty, Kazakhstan

### ABSTRACT

The article discusses the synthesis and structure of polycrystalline nanocomposite  $\text{MnCo}_2\text{O}_4\text{-GdCrO}_4$  material. The sol-gel method was used as a synthesis of the study. Using X-ray phase analysis (XPA), the structure of the synthesized nanomaterial composition was determined: spinel – cobalt manganate and perovskite – gadolinium chromite. Based on the results of the analysis, it was established that the polycrystalline two-phase composite is a system of spinel-cubic and perovskite-tetragonal types. Morphological analysis of the nanocomposite was carried out using a scanning electron microscope (SEM). According to the data obtained as a result of SEM, the elemental composition was confirmed and the average nanosize of the nanomaterial was obtained, and the content of the compound increased to x2000 was determined, the particle size of  $\text{MnCo}_2\text{O}_4$  is 383-281 nm,  $\text{GdCrO}_4$  – 1.63-1.34  $\mu\text{m}$ ; increased to x4000, particle size –  $\text{MnCo}_2\text{O}_4$  277-219 nm,  $\text{GdCrO}_4$  – 1.48-1.27  $\mu\text{m}$ ; increased to x6000, particle size –  $\text{MnCo}_2\text{O}_4$  239-209 nm,  $\text{GdCrO}_4$  – 1.21-1.07  $\mu\text{m}$ .

**Keywords:** spinel, perovskite, supercapacitor, battery, electrocatalyst, refrigerator, ferromagnetic, research, magnetocaloric, effect, parameters

### 1. Introduction

Research in multifunctional materials for advanced energy technologies aimed at overcoming major challenges in energy conversion and storage. Material development transition metal oxides have attracted attention due to their high electronegativity, rich redox reactions and high density of active sites, low cost, environmental friendliness and excellent electrochemical performance [1].

Materials with the typical chemical formula  $\text{AB}_2\text{O}_4$  spinel have gained widespread acceptance and application in the field of energy storage and storage [2], and also as electrocatalysts. Particular attention is paid to spinel materials with a bimetallic oxide structure, since they can lead to the creation of materials with higher electrochemical activity, electrical conductivity and more abundant redox reactions compared to monometallic oxides A and B [3]. Some studies report recent progress in the use of  $\text{NiCo}_2\text{O}_4$  spinels in batteries [4], supercapacitors [5], and sensors [6]. Very recently

[2] summarized the major achievements of  $\text{MCo}_2\text{O}_4$  ( $\text{M}=\text{Co, Ni, Zn, Cu, Fe and Mn}$ ) based 2D spinel materials as an integrated electrode, detailing various other nanomaterials and Co based 2D spinel materials for this applications. Current applications of  $\text{MnCo}_2\text{O}_4$  spinel are especially in energy conversion and storage. In fact, this compound has gained wide recognition as a promising, versatile and cost-effective bifunctional non-noble metal electrocatalyst due to its high redox stability, complementarity and synergy of both transition metals (manganese and cobalt), as well as efficient alternating valence states [7-10]. In addition, it is important that the supercapacitor has a suitable pore size distribution and a large specific surface area, which will reduce electrolyte consumption by regulating the porous structure and morphology of the electrode, which determines ion diffusion and conductivity, thereby affecting the capacity of the supercapacitor [11]. Various morphologies of  $\text{MnCo}_2\text{O}_4$  can be prepared and tested for suitability as a supercapacitor electrode,

\*Ответственный автор

E-mail: zhaisanbayeva.moldir@gmail.com

such as spheres [12], granular [13], nanorods [14, 15], nanosheets [16-18], cuboid microcrystals [19], nanoneedles [20], tunable porous [21], nanocages [22], network-like porous [23, 24], cubes [25, 26] and hollow spheres [27]. The use of spinel materials based on  $\text{MnCo}_2\text{O}_4$  materials for energy storage and conversion are promising components of a new concept of energy technologies. It is also important to emphasize that other applications are possible, for example, the use of  $\text{MnCo}_2\text{O}_4$ -based catalysts to convert greenhouse gases ( $\text{CO}_2$ ) and toxic gases (CO) into chemical fuels. From this perspective,  $\text{MnCo}_2\text{O}_4$ -based materials play a key role towards a more sustainable society and industrial applications.

In recent years, research into magnetocaloric materials has attracted worldwide interest due to the high potential of their use in magnetic cooling processes [28, 29]. The zircon-type ferromagnetic phase  $\text{GdCrO}_4$  is characterized by high values of magnetocaloric (MC) parameters. The effect of high MC is enhanced by polarization of  $\text{Gd}^{3+}$  ions by  $\text{Cr}^{5+}$  ions through the weaker Gd-Cr interaction. The effect should be considered when searching for new compounds with high MC effect in the range of liquid hydrogen or natural gas, concerning the liquefaction of gases by magnetization-demagnetization cycles [30]. The metal gadolinium exhibits magnetocaloric effect (MCE) through a second-order phase transition from paramagnetic to ferromagnetic (FM) at room temperature ( $T_C = 293$  K) and has been used as a cooling material in prototype magnetic refrigerators since the 1970s, starting with Brown's refrigerator [31]. However, 1997 discovered the so-called «giant FEM» in  $\text{Gd}_5\text{Si}_2\text{Ge}_2$  [32], many studies have been conducted mainly in intermetallic compounds containing rare earth elements [33]. In oxides, such examples are numerous, especially for rare earth transition metal oxides.  $\text{Gd}_3\text{Ga}_5\text{O}_{12}$  [34],  $\text{RMnO}_3$  [35],  $\text{EuR}_2\text{O}_4$  [36] and  $\text{RMn}_2\text{O}_5$  [37], where R = rare earths, have high thermal and chemical stability and exhibit large FEMs in the low-temperature region. In addition, the ferromagnetic in zircon phase  $\text{GdCrO}_4$  can be used for magnetic cooling. New families without rare earths in the composition have also been investigated as materials for cooling near room temperature [38]. Previously, Mataev et al. synthesized chromite-manganite phases by sol-gel method, the composition of which was studied by X-ray diffraction [38]. Previously, Mataev et al. synthesized chromite-manganite phases by sol-gel method, the composition of which was studied by XPA diffraction method, a single-phase composite nanomaterial was obtained [39].

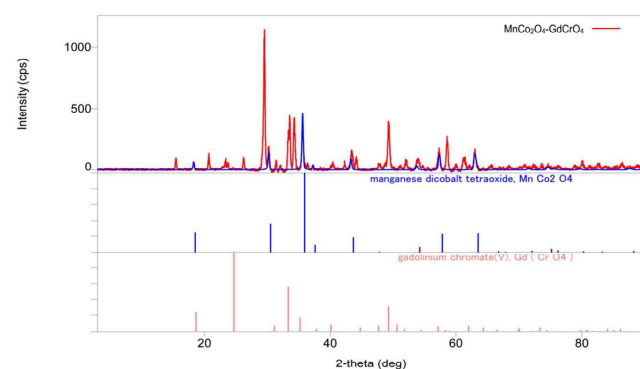


**Fig. 1.** Diffraction pattern of a polycrystalline  $\text{MnCo}_2\text{O}_4$ - $\text{GdCrO}_4$  composite.

## 2. Experimental part

### 2.1. Materials and research methods

The following starting reagents were used as materials: gadolinium (III) oxide (( $\text{Gd}_2\text{O}_3$ ), 99.99% TU 48-4-200-72, Russia); manganese (III) oxide (( $\text{Mn}_2\text{O}_3$ ), 99.99% GOST/TU 6-09-3364-78, Russia); chromium (III) oxide (( $\text{Cr}_2\text{O}_3$ ), 99% GOST TU 6-09-4272-84, Russia); cobalt (II) carbonate (( $\text{CoCO}_3$ ), 99.99% GOST 5407-78, Russia). The following equipment and measurement methods were used: an alumina crucible (diameter 50 mm (5 cm)); a Brazilian agate mortar (diameter 140 mm (14 cm)). XPA was used to determine the phase composition – using Miniflex 600 RIGAKU diffractometer ( $U=30$  kV,  $J=10$  mA, rotation speed 1000 pulses per second, time constant  $t = 5$  s, angular interval  $2\theta$  from 5 to  $90^\circ$ , Japan) and SEM JSM-6510LV JEOL (magnification  $\times 5 - \times 300,000$  (equivalent to a photo plate size of 120 mm  $\times$  90 mm); acceleration voltage: 500 V – 30 kV; resolution in high vacuum mode: 3.0 nm using

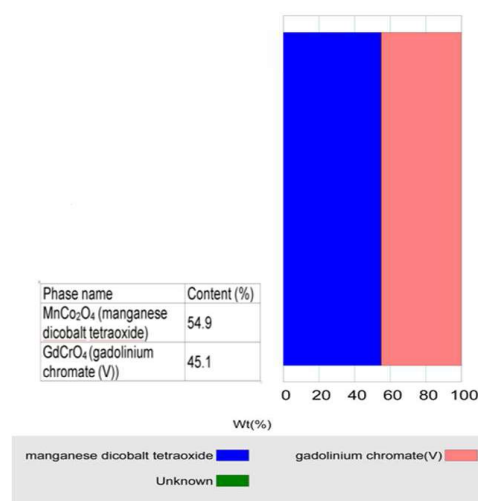


**Fig. 2.** Results of quantitative analysis of the composite.

**Table 1.** Result of quantitative analysis of the crystal lattice

Nº	Phase formula	a, Å	b, Å	c, Å	V, Å <sup>3</sup>	Space group	Z	Theor. Density(g/cm <sup>3</sup> )
1.	MnCo <sub>2</sub> O <sub>4</sub>	8.336(8)	8.336(8)	8.336(8)	579.2(10)	Fd̄-3m	8	5.418
	GdCrO <sub>4</sub>	7.587(14)	7.587(14)	6.138(14)	353.3(12)	I41	4	5.288

a tungsten cathode (at 30 kV), 8 nm (at 3 kV), 15 nm (at 1 kV); resolution in low vacuum mode: 4.0 nm (at 30 kV) Japan). Calculation and processing of 3D reconstruction surface data were performed using SEM (JEOL).

## 2.2. Synthesis – obtaining a composite nanomaterial by the sol-gel method

Two-phase MnCo<sub>2</sub>O<sub>4</sub>-GdCrO<sub>4</sub> nanomaterial synthesis was carried out by the sol-gel method. The metal oxides were doped with cobalt carbonate. The metal oxides were split in stoichiometric ratios. Citric acid and glycerin were used in the reaction as the precipitating agent, which favorably affected the formation of a homogeneous phase in the samples. Stoichiometric amounts of oxides were ground in an alumina crucible and mixed in an agate mortar until a homogeneous mixture was obtained. Distilled water, glycerin, and citric acid were added to the mixture. The mass was heated in an electric oven to obtain a gel. The resulting gel was treated in a muffle furnace at a temperature of 600 °C for 25-35 minutes. After transforming into powder, the composition was repeatedly fired, increasing the temperature in the range of 600-1100 °C. The firing was divided into six stages, with a total duration of 35 hours. After each synthesis stage, intermediate grinding and loading into the X-ray apparatus were performed. As a result of the work, a multifunctional two-phase spinel-perovskite nanocomposite was synthesized. The crystal structure of the complex oxide compound was obtained by SEM and XPA diffraction methods.

## 3. Results and discussion

The analyzed structures of the obtained spinel-perovskite nanomanganite determined its phase composition by the XPA method. The results of the XPA of the powdered polycrystalline samples showed two composites: cobalt manganate (MnCo<sub>2</sub>O<sub>4</sub>) and gadolinium chromite (GdCrO<sub>4</sub>), the ferromagnetic phase of the zircon type (Fig. 1).

In the inset of Fig. 2, a quantitative analysis of the composite is presented. The results of the quantitative analysis (internal standard method) and calibration data allowed determining that their percentage ratios

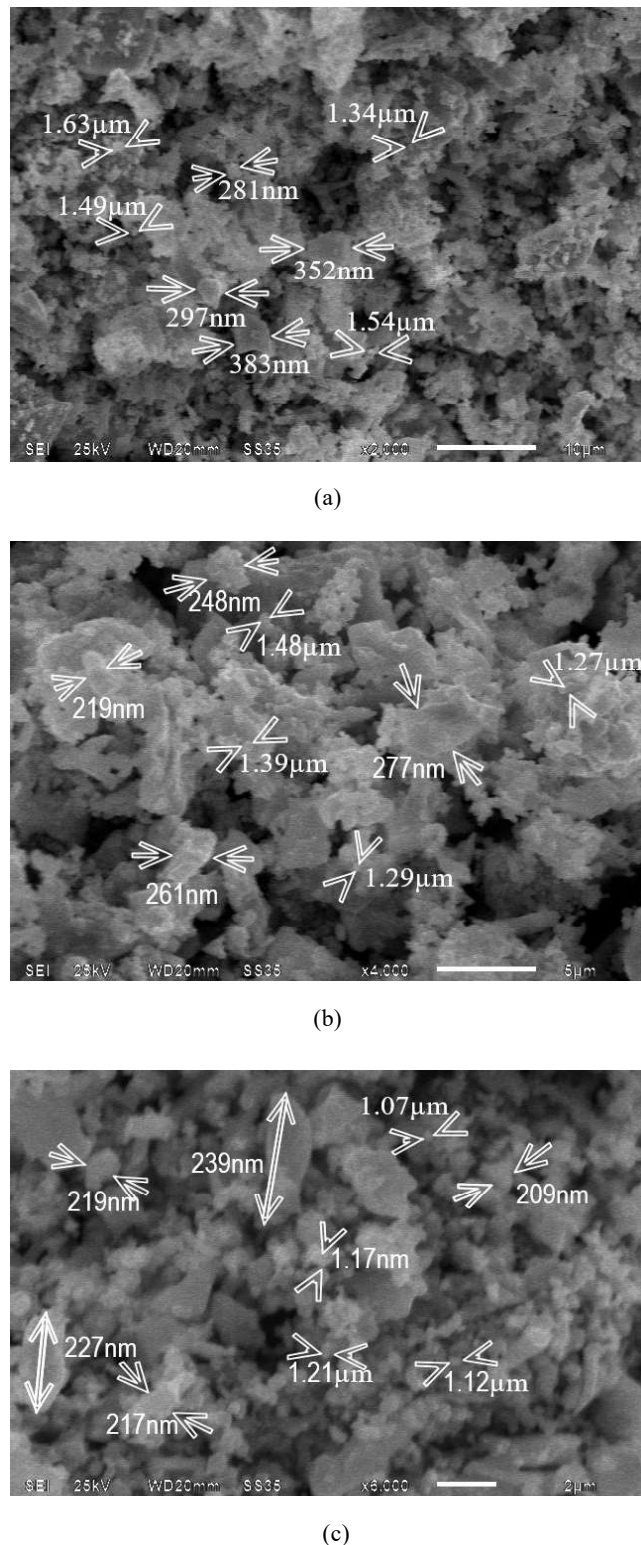


**Fig. 3.** Scanning electron microscopy increased particle size up to: (a) x2,000 MnCo<sub>2</sub>O<sub>4</sub> 383-281 nm, GdCrO<sub>4</sub> 1.63-1.34 μm; (b) x4,000 MnCo<sub>2</sub>O<sub>4</sub> 277-219 nm, GdCrO<sub>4</sub> 1.48-1.27 μm; (c) x6,000 MnCo<sub>2</sub>O<sub>4</sub> 239-209 nm, GdCrO<sub>4</sub> 1.21-1.07 μm.

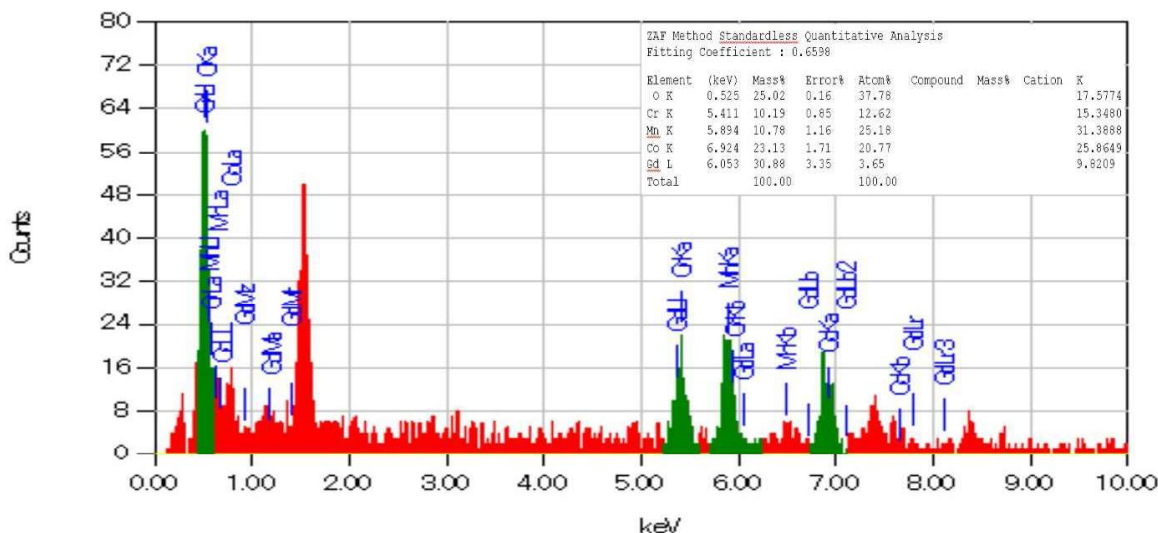


**Fig. 4.** Elemental composition of two-phase nanomaterial  $\text{MnCo}_2\text{O}_4$  -  $\text{GdCrO}_4$ .

are 54.9% for cobalt manganate ( $\text{MnCo}_2\text{O}_4$ ) and 45.1% for gadolinium chromite ( $\text{GdCrO}_4$ ).

The result of refining the structural parameters shows that the binary phase with cubic and tetragonal crystal lattice structures is presented in Table 1.

The phase  $\text{MnCo}_2\text{O}_4$  with a formula unit number  $Z=8$  crystallizes in a cubic lattice with the space group  $\text{Fd}^-3\text{m}$ . The phase  $\text{GdCrO}_4$ , respectively, with  $Z=4$  crystallizes in a tetragonal lattice with the space group  $\text{I}41$  (Table 1).

Scanning electron microscopy (JSM-6510LV JEOL) showed availability conglomerates (Fig. 3 a, b, c): increased up to  $\times 2,000$  spatial resolution 10  $\mu\text{m}$  particle size  $\text{MnCo}_2\text{O}_4$  383-281 nm,  $\text{GdCrO}_4$  1.63-1.34  $\mu\text{m}$ ; spatial resolution increased up to  $\times 4000$  5  $\mu\text{m}$  particle size  $\text{MnCo}_2\text{O}_4$  277-219 nm,  $\text{GdCrO}_4$  1.48-1.27  $\mu\text{m}$ ; spatial resolution increased

to  $\times 6000$  2  $\mu\text{m}$  particle size  $\text{MnCo}_2\text{O}_4$  239-209 nm,  $\text{GdCrO}_4$  1.21-1.07  $\mu\text{m}$ . Such dimensions particles emphasizes efficiency sol-gel synthesis in obtaining homogeneous microstructures.

Measurements of the mass of elements in a two-phase nanomaterial using scanning electron microscope data confirm that the initial composition coincides with the elemental analysis data (Fig. 4).

The 3D model generated by the SEM (JEOL) provides solutions for analytics and visualization, constructing 3D color intensity maps, anaglyphic images, profiles, and measurements of nanomaterial growth (Fig. 5). Studying the microstructure on the 3D model revealed four layers of color: the highest being red, followed by yellow, green, and blue. The images, essentially, represent a two-dimensional representation of the sample surface. SEM enables an improved understanding of complex microstructures. The metrological surface of the layers is as follows: red + 12  $\mu\text{m}$  – 24  $\mu\text{m}$ ; yellow + 10  $\mu\text{m}$  – 18.5  $\mu\text{m}$ ; green + 6.5  $\mu\text{m}$  – 24.5  $\mu\text{m}$ ; blue – 24  $\mu\text{m}$  – 28  $\mu\text{m}$ .

This 3D image is intuitive understandable and possible calculate characteristics surfaces. The most high from the surface (red layers) +12  $\mu\text{m}$ , the most deep (blue layers) – 28  $\mu\text{m}$ . The results of the structural analysis expand the database of nanocomposite materials with promising electrophysical properties.

#### 4. Conclusion

The phase structure and morphological analysis were carried out using SEM of the resulting two-phase nanomaterial. According to the results of the study, the crystallographic results confirmed that the types of two-phase polycrystals are cubic and tetragonal

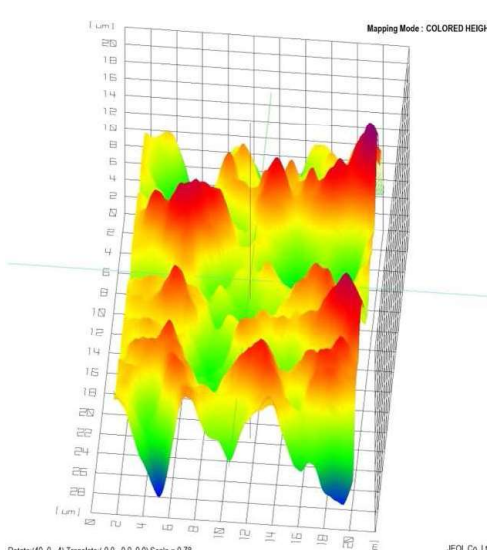


**Fig. 5.** P E M - 3D surface reconstruction.

lattice system. With formula units of the amount of cobalt manganate  $Z=8$ , it is determined that the shape parameter of the cubic unit cell is  $a,b,c=8.336 \text{ \AA}$ , and the tetragonal gadolinium chromite compound  $Z=4$ , the unit cell parameter is  $a=7.587 \text{ \AA}$ ,  $b=7.587 \text{ \AA}$ ,  $c=6.138 \text{ \AA}$ . Also, by determining the cell volumes of  $\text{MnCo}_2\text{O}_4=579.2 \text{ \AA}^3$ ,  $\text{GdCrO}_4=353.3 \text{ \AA}^3$ , the formation of nanoscale product and its elemental composition were proved.

## References

- [1]. Uke S.J., Akhare V.P., Bambole D.R. Recent advancements in the cobalt oxides, manganese oxides, and their composite as an electrode material for Supercapacitor: a review // *Frontiers in Materials*. – 2017. – Vol. 4.
- [2]. Zhao X., Mao L., Cheng Q. Two-dimensional spinel structured co-based materials for high performance supercapacitors: a critical review // *Chemical Engineering Journal*. – 2020. – Vol. 387. – P.124081.
- [3]. Li Y., Xiao H., Yi T. Review and prospect of  $\text{NiCo}_2\text{O}_4$ -based composite materials for supercapacitor electrodes // *Journal of Energy Chemistry*. – 2019. – Vol. 31. – P.54-78.
- [4]. Xiao H., Gui X., Yi T. Recent progress of  $\text{NiCo}_2\text{O}_4$ -based anodes for high-performance lithium-ion batteries // *Current Opinion in Solid State & Materials Science*. – 2018. – Vol. 4(22). – P.109-126.
- [5]. Cheng J.P., Wang W.D., Wang X.C. Recent research of core-shell structured composites with  $\text{NiCo}_2\text{O}_4$  as scaffolds for electrochemical capacitors // *Chemical Engineering Journal*. – 2020. – Vol. 393. – P.124747.
- [6]. Kumar R.  $\text{NiCO}_2\text{O}_4$  Nano-/Microstructures as High-Performance Biosensors: A Review // *Nano-Micro Letters*. – 2020. – Vol. 1(12).
- [7]. Yuvaraj S., Ahilan V., Shammugam S. Nitrogen-doped Multi-walled Carbon Nanotubes- $\text{MnCo}_2\text{O}_4$  microsphere as electrocatalyst for efficient oxygen reduction reaction // *International Journal of Hydrogen Energy*. – 2016. – Vol. 34(41). – P.15199-15207.
- [8]. Oh T.I., Ryu S.G., Oh H.-W.  $\text{MnCo}_2\text{O}_4$  nanoparticles supported on nitrogen and sulfur co-doped mesoporous carbon spheres as efficient electrocatalysts for oxygen catalytic reactions // *Dalton Transactions*. – 2019. – Vol. 3(48). – P.945-953.
- [9]. Yang H., Zhu M., Guo X. Anchoring  $\text{MnCo}_2\text{O}_4$  Nanorods from Bimetal-Organic Framework on rGO for High-Performance Oxygen Evolution and Reduction Reaction // *ACS Omega*. – 2019. – Vol. 27(4). – P.22325-22331.
- [10]. Lin Y., Liu Y., Cao D. Electro-deposition of nickel-iron nanoparticles on flower-like  $\text{MnCo}_2\text{O}_4$  nanowires as an efficient bifunctional electrocatalyst for overall water splitting // *CrystEngComm*. – 2020. – Vol. 8(22). – P.1425-1435.
- [11]. Gonçalves J.M., Silva M.N.T., Naik K.K. Multifunctional spinel  $\text{MnCo}_2\text{O}_4$  based materials for energy storage and conversion: a review on emerging trends, recent developments and future perspectives // *Journal of Materials Chemistry. A, Materials for Energy and Sustainability*. – 2021. – Vol. 6(9). – P.3095-3124.
- [12]. Gao Y., Xia Y., Wan H. Enhanced cycle performance of hierarchical porous sphere  $\text{MnCo}_2\text{O}_4$  for asymmetric supercapacitors // *Electrochimica Acta*. – 2019. – Vol. 301. – P.294-303.
- [13]. Kong L., Lü C., Liu M. The specific capacitance of sol-gel synthesised spinel  $\text{MnCo}_2\text{O}_4$  in an alkaline electrolyte // *Electrochimica Acta*. – 2014. – Vol. 115. – P.22-27.
- [14]. Venkatachalam V., Alsalmi A., Alghamdi A. High performance electrochemical capacitor based on  $\text{MnCo}_2\text{O}_4$  nanostructured electrode // *Journal of Electroanalytical Chemistry*. – 2015. – Vol. 756. – P.94-100.
- [15]. Xu J., Sun Y., Lu M. Fabrication of the porous  $\text{MnCo}_2\text{O}_4$ nanorodarrays on Ni foam as an advanced electrode for asymmetric supercapacitors // *Acta Materialia*. – 2018. – Vol. 152. P.162-174.
- [16]. Sahoo S., Naik K.K., Rout C.S. Electrodeposition of spinel  $\text{MnCo}_2\text{O}_4$  nanosheets for supercapacitor applications // *Nanotechnology*. – 2015. – Vol. 45(26). – P.455401.
- [17]. Nagamuthu S., Vijayakumar S., Lee S. Hybrid supercapacitor devices based on  $\text{MnCo}_2\text{O}_4$  as the positive electrode and  $\text{FeMn}_2\text{O}_4$  as the negative electrode // *Applied Surface Science*. – 2016. – Vol. 390. – P. 202-208.
- [18]. Li J., Xiong D., Wang L. High-performance self-assembly  $\text{MnCo}_2\text{O}_4$  nanosheets for asymmetric supercapacitors // *Journal of Energy Chemistry*. – 2019. – Vol. 37. – P. 66-72.
- [19]. Krishnan S.G., Hasbi Ab.R.M., Jose R. Synthesis and characterization of  $\text{MnCo}_2\text{O}_4$  cuboidal microcrystals as a high performance pseudocapacitor electrode // *Journal of Alloys and Compounds*. – 2016. – Vol. 656. – P.707-713.
- [20]. Hui K.N., Hui K.S., Tang Z. Hierarchical chestnut-like  $\text{MnCo}_2\text{O}_4$  nanoneedles grown on nickel foam as binder-free electrode for high energy density asymmetric supercapacitors // *Journal of Power Sources*. – 2016. – Vol. 330. – P.195-203.
- [21]. Akhtar Md.A., Sharma V., Biswas S. Tuning porous nanostructures of  $\text{MnCo}_2\text{O}_4$ for application in supercapacitors and catalysis // *RSC Advances*. – 2016. – Vol. 98(6). – P.96296-96305.
- [22]. Dong Y., Wang Y., Xu Y., Facile synthesis of hierarchical nanocage  $\text{MnCo}_2\text{O}_4$  for high performance supercapacitor // *Electrochimica Acta*. – 2017. – Vol. 225. – P.39-46.
- [23]. Huang T.-C., Zhao C., Lin-Hua W. 3D network-

- like porous MnCo<sub>2</sub>O<sub>4</sub> by the sucrose-assisted combustion method for high-performance supercapacitors // Ceramics International. – 2017. – Vol. 2(43). – P.1968-1974.
- [24]. Shanmugavadiel M., Dhayabaran V.V., Subramanian M. Fabrication of high energy and high power density supercapacitor based on MnCo<sub>2</sub>O<sub>4</sub> nanomaterial // Journal of Physics and Chemistry of Solids. – 2019. – Vol. 133. – P.15-20.
- [25]. Sannasi V., Karuppuchamy S. High-pseudocapacitance of MnCo<sub>2</sub>O<sub>4</sub> nanostructures prepared by phenolphthalein assisted hydrothermal and microwave methods // Ceramics International. – 2020. – Vol. 10(46). – P.15510-15520.
- [26]. Li M., Yang W., Li J. Porous layered stacked MnCo<sub>2</sub>O<sub>4</sub> cubes with enhanced electrochemical capacitive performance // Nanoscale. – 2018. – Vol. 5(10). – P. 2218-2225.
- [27]. Liu Z., Teng F., Chen Y. Highly uniform MnCo<sub>2</sub>O<sub>4</sub> hollow Spheres-Based All-Solid-State asymmetric Micro-Supercapacitor via a simple Metal-Glycerate precursor approach // Energy Technology. – 2019. – Vol. 9(7).
- [28]. Yu B., Gao Q., Zhang B. Review on research of room temperature magnetic refrigeration // International Journal of Refrigeration. – 2003. – Vol. 6(26). – P.622-636.
- [29]. GschneidnerJr K.A., Pecharsky V.K., Tsokol A.O. Recent developments in magnetocaloric materials // Reports on Progress in Physics. – 2005. – Vol. 6 (68). – P.1479-1539.
- [30]. Palacios E., Tomasi C., Sáez-Puche R. Effect of Gd polarization on the large magnetocaloric effect of GdCrO<sub>4</sub> in a broad temperature range // Physical Review. – 2016. – Vol. 6(93).
- [31]. Brown G.V. Magnetic heat pumping near room temperature // Journal of Applied Physics. – 1976. – Vol. 8(47). – P.3673-3680.
- [32]. Pecharsky V.K., Gschneidner K.A. Giant Magnetocaloric Effect In Gd<sub>5</sub>(Si<sub>2</sub>Ge<sub>2</sub>) // Physical Review Letters. – 1997. – Vol. 23(78). – P.4494-4497.
- [33]. Khmelevskyi S., Mohn P. The order of the magnetic phase transitions in RCo<sub>2</sub>(R = rare earth) intermetallic compounds // Journal of Physics: Condensed Matter. – 2000. – Vol. 45(12). – P.9453-9464.
- [34]. Tishin A.M., Spichkin Y.I. The Magnetocaloric Effect and its Applications / A.M. Tishin, Y.I. Spichkin. – 2016.
- [35]. Cheong S., Mostovoy M. Multiferroics: a magnetic twist for ferroelectricity // Nature Materials. – 2007. – Vol. 1(6). – P.13-20.
- [36]. Midya A., Khan N., Bhoi D. Giant magnetocaloric effect in magnetically frustrated EuHo<sub>2</sub>O<sub>4</sub> and EuDy<sub>2</sub>O<sub>4</sub> compounds // Applied Physics Letters. – 2012. – Vol. 13(101).
- [37]. Balli M., Jandl S., Fournier P. Anisotropy-enhanced giant reversible rotating magnetocaloric effect in HoMn<sub>2</sub>O<sub>5</sub> single crystals // Applied Physics Letters. – 2014. – Vol. 23(104).
- [38]. Franco V., Blázquez J.S., Ingale B. The magnetocaloric effect and magnetic refrigeration near room temperature: Materials and models // Annual Review of Materials Research. – 2012. – Vol. 1(42).– P.305-342.
- [39]. Mataev M.M., Patrin G.S., Seitbekova K. Zh., Tursinova Zh.Y., Abdraimova M. R. Synthesis and X-ray dif fraction study of the chromite-manganites // Chemical journal of Kazakhstan. – 2019. – P.207-216.

## References

- [1]. Uke SJ, Akhare VP, Bambole DR, Bodade AB, & Chaudhari GN (2017) Frontiers in Materials 4. <https://doi.org/10.3389/fmats.2017.00021>
- [2]. Zhao X, Mao L, Cheng Q, Li J, Liao F, Yang G, Xie L, Zhao C, & Chen L (2020) Chemical Engineering Journal 387:124081. <https://doi.org/10.1016/j.cej.2020.124081>
- [3]. Li Y, Xiao H, Yi T, He Y, & Li X (2019) Journal of Energy Chemistry 31:54-78. <https://doi.org/10.1016/j.jecchem.2018.05.010>
- [4]. Xiao H, Gui X, Yi T, Li Y, & Yue C (2018) Current Opinion in Solid State & Materials Science 22(4): 109-126. <https://doi.org/10.1016/j.cossms.2018.05.005>
- [5]. Cheng J, Wang W, Wang X, & Liu F (2020) Chemical Engineering Journal 393:124747. <https://doi.org/10.1016/j.cej.2020.124747>
- [6]. Kumar R (2020) Nano-Micro Letters 12:1. <https://doi.org/10.1007/s40820-020-00462-w>
- [7]. Yuvaraj S, Ahilan V, Shanmugam S, & Selvan RK (2016) International Journal of Hydrogen Energy 41(34):15199-15207. <https://doi.org/10.1016/j.ijhydene.2016.06.115>
- [8]. Oh TI, Ryu SG, & Oh H (2019) Dalton Transactions 48(3):945-953. <https://doi.org/10.1039/c8dt03955k>
- [9]. Yang H, Zhu M, Guo X, Yan C, & Lin S (2019) ACS Omega 4(27):22325–22331. <https://doi.org/10.1021/acsomega.9b02362>
- [10]. Lin Y, Liu Y, Cao D, & Gong Y (2020) CrystEngComm 22(8):1425-1435. <https://doi.org/10.1039/c9ce01921a>
- [11]. Gonçalves JM, Silva MNT, Naik KK, Martins PR, Rocha DP, Nossol E, Muñoz RA, Angnes L, & Rout CS (2021) Journal of Materials Chemistry A Materials for Energy and Sustainability 9(6):3095-3124. <https://doi.org/10.1039/d0ta11129e>
- [12]. Gao Y, Xia Y, Wan H, Xu X, & Jiang S (2019) Electrochimica Acta 301:294–303. <https://doi.org/10.1016/j.electacta.2019.01.173>
- [13]. Kong L, Lü C, Liu M, Luo Y, Kang L, Li X, & Walsh FC (2014) Electrochimica Acta 115:22-27. <https://doi.org/10.1016/j.electacta.2013.10.089>
- [14]. Venkatachalam V, Alsalmi A, Alghamdi A, Jayavel R (2015). Journal of Electroanalytical

- Chemistry 756:94-100. <https://doi.org/10.1016/j.jelechem.2015.08.019>
- [15]. Xu J, Sun Y, Lu M, Wang L, Zhang J, Qian J, & Liu X (2018) Acta Materialia 152:162-174. <https://doi.org/10.1016/j.actamat.2018.04.025>
- [16]. Sahoo S, Naik KK, & Rout CS (2015) Nanotechnology 26(45):455401. <https://doi.org/10.1088/0957-4484/26/45/455401>
- [17]. Nagamuthu S, Vijayakumar S, Lee S, & Ryu K (2016) Applied Surface Science 390:202-208. <https://doi.org/10.1016/j.apsusc.2016.08.072>
- [18]. Li J, Xiong D, Wang L, Sari HMK, & Li X (2019) Journal of Energy Chemistry 37:66-72. <https://doi.org/10.1016/j.jecchem.2018.11.015>
- [19]. Krishnan SG, Hasbi ARM, & Jose R (2016) Journal of Alloys and Compounds 656: 707-713. <https://doi.org/10.1016/j.jallcom.2015.10.007>
- [20]. Hui KN, Hui KS, Tang Z, Jadhav VV, & Xia QX (2016) Journal of Power Sources 330:195-203. <https://doi.org/10.1016/j.jpowsour.2016.08.116>
- [21]. Akhtar MA, Sharma V, Biswas S, & Chandra A (2016) RSC Advances 6(98):96296-96305. <https://doi.org/10.1039/c6ra20004d>
- [22]. Dong Y, Wang Y, Xu Y, Chen C, Wang Y, Jiao L, & Yuan H (2017) Electrochimica Acta 225:39-46. <https://doi.org/10.1016/j.electacta.2016.12.109>
- [23]. Huang T, Zhao C, Lin-Hua W, Lang X, Liu K, & Zhang H (2017) Ceramics International 43(2):1968-1974. <https://doi.org/10.1016/j.ceramint.2016.10.162>
- [24]. Shanmugavadiel M, Dhayabaran VV, & Subramanian M (2019) Journal of Physics and Chemistry of Solids 133:15-20. <https://doi.org/10.1016/j.jpcs.2019.04.029>
- [25]. Sannasi V & Karuppuchamy S (2020) Ceramics International 46(10):15510-15520. <https://doi.org/10.1016/j.ceramint.2020.03.096>
- [26]. Li M, Yang W, Li J, Feng M, Li W, & Li H (2018) Nanoscale 10(5):2218-2225. <https://doi.org/10.1039/c7nr08239h>
- [27]. Liu Z, Teng F, Chen Y, Abideen ZU, Gu W & Liu Z (2019) Energy Technology 7(9). <https://doi.org/10.1002/ente.201900314>
- [28]. Yu B, Gao Q, Zhang B, Meng X, Chen Z (2003) International Journal of Refrigeration 26(6):622-636. [https://doi.org/10.1016/s0140-7007\(03\)00048-3](https://doi.org/10.1016/s0140-7007(03)00048-3)
- [29]. GschneidnerJr KA, Pecharsky VK, & Tsokol AO (2005) Reports on Progress in Physics 68(6):1479-1539. <https://doi.org/10.1088/0034-4885/68/6/r04>
- [30]. Palacios E, Tomasi C, Sáez-Puche R, santos-García AJD, Fernández-Martínez F, Burriel R (2016) Physical Review 93(6). <https://doi.org/10.1103/physrevb.93.064420>
- [31]. Brown GV (1976). Journal of Applied Physics 47(8):3673-3680. <https://doi.org/10.1063/1.323176>
- [32]. Pecharsky VK, & Gschneidner KA (1997) Physical Review Letters 78(23): 4494-4497. <https://doi.org/10.1103/physrevlett.78.4494>
- [33]. Khmelevskyi S, Mohn P (2000) Journal of Physics: Condensed Matter 12(45):9453-9464. <https://doi.org/10.1088/0953-8984/12/45/308>
- [34]. Tishin A, Spichkin Y (2016) In CRC Press eBooks. <https://doi.org/10.1201/9781420033373>
- [35]. Cheong S, Mostovoy M (2007) Nature Materials 6(1):13-20. <https://doi.org/10.1038/nmat1804>
- [36]. Midya A, Khan N, Bhoi D, Mandal P (2012) Applied Physics Letters 101(13). <https://doi.org/10.1063/1.4754849>
- [37]. Balli M, Jandl S, Fournier P, Gospodinov M (2014) Applied Physics Letters 104(23). <https://doi.org/10.1063/1.4880818>
- [38]. Franco V, Blázquez J, Ingale B, Conde A (2012) Annual Review of Materials Research 42(1): 305-342. <https://doi.org/10.1146/annurev-matsci-062910-100356>
- [39]. Mataev MM, Patrin GS, Seitbekova KZh, Tursinova ZhY, Abdraimova MR (2019) Chemical journal of Kazakhstan: 207-216. ISSN 1813-1107

## MnCo<sub>2</sub>O<sub>4</sub>-GdCrO<sub>4</sub> поликристалдарының синтезі және құрылымы

М.М. Матаев<sup>1</sup>, Г.С. Патрин<sup>2</sup>, А.А. Мельдешов<sup>1</sup>, К.Ж. Сейтбекова<sup>3</sup>, М.Е. Жайсанбаева<sup>1\*</sup>

<sup>1</sup>Қазақ Ұлттық Қыздар Педагогикалық Университеті, Гоголя к-си, 114к1, Алматы, Қазақстан

<sup>2</sup>Сібір федералды университеті, Свободный даңғылы, 79, Красноярск, Ресей

<sup>3</sup>Абай атындағы Қазақ ұлттық педагогикалық университеті, Достық даңғылы, 13, Алматы, Қазақстан

## АНДАТПА

Мақалада поликристалды нанокомпозиттік MnCo<sub>2</sub>O<sub>4</sub>-GdCrO<sub>4</sub> материалының синтезі мен құрылымы қарастырылады. Зерттеудің синтезі ретінде золь-гель әдісі қолданылды. Рентгендік фазалық талдау (РФА) көмегімен синтезделген наноматериал құрамы анықталды: шпинель - кобальт манганингаты және перовскит - гадолиний хромит. Талдау нәтижелері бойынша поликристалды екі фазалы композиттің шпинельді-кубышқа және перовскит-тетрагональды типті жүйе екендігі анықталды. Нанокомпозиттің морфологиялық талдауы сканерлеуші электронды микроскоптың (СЭМ) көмегімен жүргізілді. СЭМ нәтижесінде алынған мәліметтер бойынша элементтік құрамы расталды және наноматериалдың орташа наноөлемі алынды, қосылыстың мөлшері анықталып болшектердің өлшемі x2000 дейін ұлгайғанда MnCo<sub>2</sub>O<sub>4</sub> 383-281 нм (nm), GdCrO<sub>4</sub> 1.63-1.34 мкм

( $\mu\text{m}$ ); бөлшектердің өлшемі  $x4000$  ұлғайғанда  $\text{MnCo}_2\text{O}_4$  277-219 нм (nm),  $\text{GdCrO}_4$  1.48-1.27 мкм ( $\mu\text{m}$ ); бөлшектердің өлшемі  $x6000$  ұлғайғанда  $\text{MnCo}_2\text{O}_4$  239-209 нм (nm),  $\text{GdCrO}_4$  1.21-1.07 мкм ( $\mu\text{m}$ ) дейін өсті.

*Түйін сөздер:* Шпинель, перовскит, суперконденсатор, аккумулятор, электрокатализатор, тоңазытқыш, ферромагниттік, зерттеу, магнитокалориялық, эффект, параметрлер

### **Синтез и структура поликристаллов $\text{MnCo}_2\text{O}_4$ - $\text{GdCrO}_4$**

М.М. Матаев<sup>1</sup>, Г.С. Патрин<sup>2</sup>, А.А. Мельдешов<sup>1</sup>, К.Ж. Сейтбекова<sup>3</sup>, М.Е. Жайсанбаева<sup>1\*</sup>

<sup>1</sup>Казахский национальный женский педагогический университет, ул. Гоголя, 114 к1, Алматы, Казахстан

<sup>2</sup>Сибирский федеральный университет, пр. Свободный, 79, Красноярск, Россия

<sup>3</sup>Казахский национальный педагогический университет им. Абая, пр. Достык, 13, Алматы, Казахстан

### **АННОТАЦИЯ**

В статье рассмотрены синтез и структура поликристаллического нанокомпозитного  $\text{MnCo}_2\text{O}_4$ - $\text{GdCrO}_4$  материала, полученного методом золь-гель. Методом рентгенофазового анализа (РФА) определена структура синтезированной

композиции наноматериала: шпинель – мanganat кобальта и перовскит – хромит гадолиния. По результатам анализа установлено, что поликристаллический двухфазный композит представляет собой сингонию шпинель-кубического и перовскит-тетрагонального типов. Морфологический анализ нанокомпозита проводился с помощью сканирующего электронного микроскопа (СЭМ). По данным, полученным в результате СЭМ, подтверждён элементный состав и определены средний наноразмер наноматериала, а также содержание соединения, увеличенного до  $x2000$ , размер частиц  $\text{MnCo}_2\text{O}_4$  – 383-281 нм,  $\text{GdCrO}_4$  – 1.63-1.34 мкм; увеличенного до  $x4000$ , размер частиц –  $\text{MnCo}_2\text{O}_4$  277-219 нм,  $\text{GdCrO}_4$  – 1.48-1.27 мкм; увеличенного до  $x6000$ , размер частиц –  $\text{MnCo}_2\text{O}_4$  239-209 нм,  $\text{GdCrO}_4$  – 1.21-1.07 мкм.

*Ключевые слова:* шпинель, перовскит, суперконденсатор, батарея, электрокатализатор, ходильник, ферромагнитная, исследования, магнитокалорических, эффект, параметры